Proc. Natl. Acad. Sci. USA
Vol. 91, pp. 10586–10590, October 1994
Neurobiology

Rhythmogenesis, amplitude modulation, and multiplexing in a cortical architecture

NANCY KOPELL* AND GWENDAL LEMASSON†‡

*Department of Mathematics, Boston University, Boston, MA 02215; †Center for Complex Systems, Brandeis University, Waltham, MA 02254; and ‡Laboratoire de Neurobiologie et Physiologie Comparee, Université de Bordeaux, 33120 Arcachon, France

Communicated by Louis N. Howard, June 20, 1994 (received for review July 6, 1993)

ABSTRACT **In a network of excitatory and inhibitory neurons, hyperpolarization-activated inward currents can help to produce population rhythms in which individual cells participate sparsely and randomly. A shift in the activation curve of such a current changes the fraction of the cells participating in any given cycle of the population rhythm, thus changing the amplitude of the field potential. Furthermore, the frequency of the population rhythm remains relatively fixed over a substantial range of amplitudes, allowing the population rhythm to play a separate processing role from that of the individual components.**

Neurons in the central nervous system have many different ionic currents that contribute to their behavior and to the emergent behavior of the network of such neurons (1). It is of interest to understand the functional significance of different currents and combinations of them. The hyperpolarization-activated cation current i_h has been found in a variety of cells and preparations in the central nervous system (2–12). This current is very small when the cell is depolarized, but it has important effects on the activity of the neuron when the cell is hyperpolarized. It has been suggested that i_h helps set the resting potential of a cell, thereby modulating the effects of other currents (2, 3) and that it is significant in producing and modulating rhythmic activity in a single cell (3, 4). It is known that i_h can be modulated by histamine (5), noradrenaline (4, 6), serotonin (6), the volatile anesthetics enflurane and forskolin (7), nitric oxide (8), and cyclic AMP (9) by shifting the activation curve of i_h in either the hyperpolarized or the depolarized direction. This modulation has been suggested to play a role in the ability of the thalamocortical relay cells to switch behavior between low-frequency rhythmic bursting characteristic of the sleep state and the more excitable but less regular behavior characteristic of the waking state (3, 4, 10).

We suggest another function that hyperpolarization-activated currents may be playing in general cortical-like tissue that produces rhythmic output (13). We show via simulations that if i_h is present along with standard Hodgkin–Huxley sodium and potassium channels, population rhythms can be obtained from model cells, none of which are themselves capable of oscillation (burst or tonic firing) without external input. In these population rhythms, individual cells fire action potentials only infrequently (14–16). Shifting the activation curve of i_h or changing its maximal conductance in some of the cells modulates the amplitude of the population rhythm; if i_h is increased, by increasing the maximal conductance or shifting the activation curve in the depolarized direction, more excitatory cells fire within a cycle, giving a range of amplitudes for the associated field potential. In our simulations, the frequency of the population remains relatively fixed over a substantial range of amplitudes. Since the rhythm of the population can continue without change when a given microcircuit is withdrawn, the i_h modulation provides a mechanism by which a microcircuit and the global oscillation can perform different processing tasks (multiplexing).

We illustrate our points by using a relatively simple network, in which each of the cells is described by voltage-gated conductance equations with a small number of ionic currents. As in cortical tissue, there is substantial convergence and divergence of connections. The model cells are connected to one another via excitatory or inhibitory synapses.

With some changes in parameters, the ionic conductances and synapses that we use suffice to produce an oscillation even for a single pair of excitatory and inhibitory cells. However, a large number of neurons is needed to get a rhythm in which each cell fires less often than once per "field potential" cycle, and a very large network is required for very sparse participation. We describe our simulations in networks of many cells and then explain the results by using simulations and analysis of behavior in smaller networks.

Simulations and Results

Simulations were carried out in a network consisting of 55 elements, each described by voltage-gated conductance equations similar to the Hodgkin–Huxley equations. Each cell had a fast sodium current with an activation and inactivation, a slower potassium current, and a leak current. In addition, the 50 cells designated excitatory cells (E-cells) were each given a hyperpolarization-activated inward current (i_h). This current activates slowly in the hyperpolarized regime and deactivates more quickly in the depolarized regime. The other 5 cells were designated inhibitory cells (I-cells). Without connections to other cells, each cell remained at resting potential. (In the presence of sufficient depolarizing injected current, they would fire periodically.) The cells were identical except for the maximal conductance of i_h. The equations used are in the *Appendix*.

Each E-cell was connected to two I-cells, with connections randomly chosen. Each I-cell was connected to 10 E-cells, again with the connections random. There were no connections from E-cells to E-cells or I-cells to I-cells. The connections were modeled by using caricatures of voltage-gated excitatory and inhibitory synapses, also given in the *Appendix*. The model inhibitory synapses (i.e., the connection from an I-cell to E-cell) were slower than the model excitatory synapses (connections from E-cells to I-cells).

A series of simulations was run using different values for the maximal conductance of i_h and different positions of the activation curve. The network was started by stimulating a fraction of the cells for a short time. If the average amount of i_h in the system was too small, the network returned to rest shortly after the end of stimulation. If the amount of i_h was very large, we obtained rhythms in which each cell fired in

The publication costs of this article were defrayed in part by page charge payment. This article must therefore be hereby marked "*advertisement*" in accordance with 18 U.S.C. §1734 solely to indicate this fact.

Abbreviations: E-cell, excitatory cell; I-cell, inhibitory cell; IPSP, inhibitory postsynaptic potential.

every period of the oscillation. For intermediate cases, we illustrate our major findings in Fig. 1.

Fig. 1 shows voltage vs. time for 3 of 5 of the I-cells and 25 of 50 of the E-cells. The last trace at the bottom of each graph is a computation of the field potential. (To obtain an analogue of the field potential, the cells were placed arbitrarily in a two-dimensional grid. The calculated quantity is proportional to the sum of all the currents for each cell and inversely proportional for each cell to the distance to the electrode. The qualitative behavior was the same for different positions of the electrode.) The graphs are taken from a portion of a run after the initial stimulation was removed. In each case, the maximal conductance of i_h varies among the E-cells, between 0.03 and 0.3 mS/cm^2, using a uniform distribution with a mean of 0.17 and a SD of 0.069. The parameters in Fig. 1*B* are those of Fig. 1*A*, with the activation curve of i_h displaced in the depolarizing direction, with half-activation changed from −75 to −65 mV.

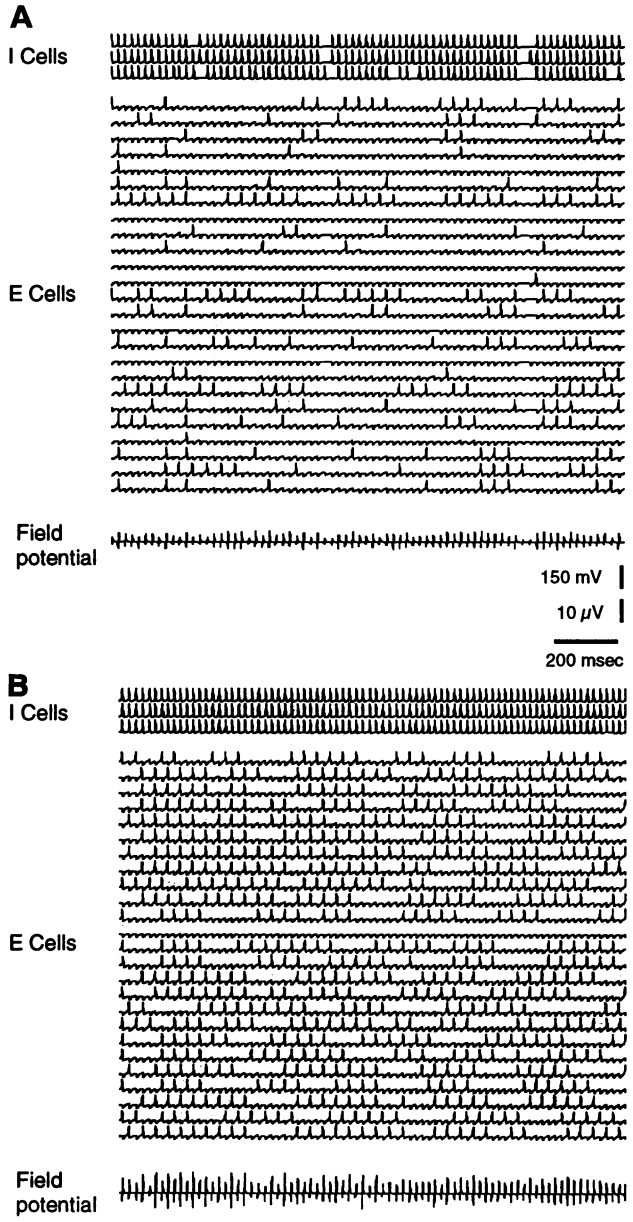

FIG. 1. Network with 50 E-cells and 5 I-cells. The E-cells have an i_h current whose activation curve is a saturating sigmoidal function decreasing with increasing voltage. (*A*) Spontaneous activity of network with half-activation of i_h in the E-cells set to −75 mV. Field potential is rhythmic with an average frequency of 46 Hz. (*B*) Spontaneous activity of network with half-activation of i_h in the E-cells set to −65 mV. Fraction of cycles in which each cell fires is increased and the field potential amplitude is higher, but the population frequency is approximately the same (49 Hz).

The following features of these figures held in all of the simulations: (*i*) There is a fairly regular rhythmic activity that is not perfectly periodic. (*ii*) Individual cells, especially E-cells, fire far less frequently than once per cycle and in a manner that is seemingly random. In particular, there is no obvious longer periodicity for an individual cell. (*iii*) If the activation curve of i_h in the E-cells is displaced in the depolarized direction, the E-cells fire on the average more often. This is also true if the mean maximal conductance of i_h in the E-cells is increased. (*iv*) The population period does not change substantially with the change in i_h level. Rather, the field potential increases with the increase in i_h conductance.

Role of Some Rate Constants

A network consisting of one E-cell and one I-cell is capable of producing a rhythmic firing, using the postsynaptic rebound exhibited by the E-cell (17). The firing of the E-cell quickly induces an action potential in the I-cell. The resulting inhibitory postsynpatic potential (IPSP) in the E-cell turns on i_h in the E-cell, and this cell then fires when released sufficiently from inhibition by the decay of the inhibitory synaptic current. This mechanism differs from others that produce oscillations from an ensemble of excitatory and inhibitory cells (18–20).

The phenomenon of postinhibitory rebound can be exhibited even without i_h. However, in that case, after an IPSP too small to elicit a rebound, the system moves toward its previous resting potential. Unless the IPSPs come too quickly for the system to return close to that potential, the system has no memory. By contrast, with i_h, an IPSP too small to provoke a rebound can turn on i_h, which does not inactivate between pulses. When another IPSP is later received, it arrives when the cell is closer to threshold and can exhibit rebound with the same IPSP that was previously too small. When the cell is depolarized, i_h decays quickly, so the response ends after one firing and the cell can again build up slowly. This mechanism is capable of producing one response after many inhibitory impulses. Furthermore, it can do so in a step-like manner as parameters are changed (21–23).

The population oscillation is due to a combination of effects: i_h allows each cell to fire after several IPSPs; the I-cell fires, as in the 2-cell circuit with 1 E-cell and 1 I-cell, provided that at least 1 E-cell fires at each cycle and thereby gives excitation to the I-cell. The requirement that at least 1 E-cell fire per cycle implies that the fraction of cycles in which each cell fires cannot be very low for a small network.

To clarify the role of i_h and rate constants in the mechanism, we use a network of intermediate size: 6 E-cells and 1 I-cell to which all the E-cells are connected. With appropriate values of maximal conductance and half-activation voltage of i_h, the population of E-cells splits into several subpopulations, with each E-cell firing once for several population cycles. In Fig. 2 *A* and *B*, we plot the voltage, i_h conductance, and inhibitory synaptic conductance as functions of time for a single E-cell. Arrowheads mark the onset of I-cell firing. Note that the conductance of i_h builds up with each successive IPSP and resets rapidly when the cell fires. The conductance of the inhibitory synaptic current increases shortly after the E-cell fires, reflecting the short interval between the firing of some E-cells and the subsequent firing of the I-cell. The longer decay time of the inhibitory conductance appears to be the most important variable in setting the frequency of the network rhythm. Fig. 2 *B* and *C* illustrates that a change in the kinetics of the inhibition has a significant effect on the period of the rhythm. Fig. 2 *A* and *D* shows that a change in the kinetics of

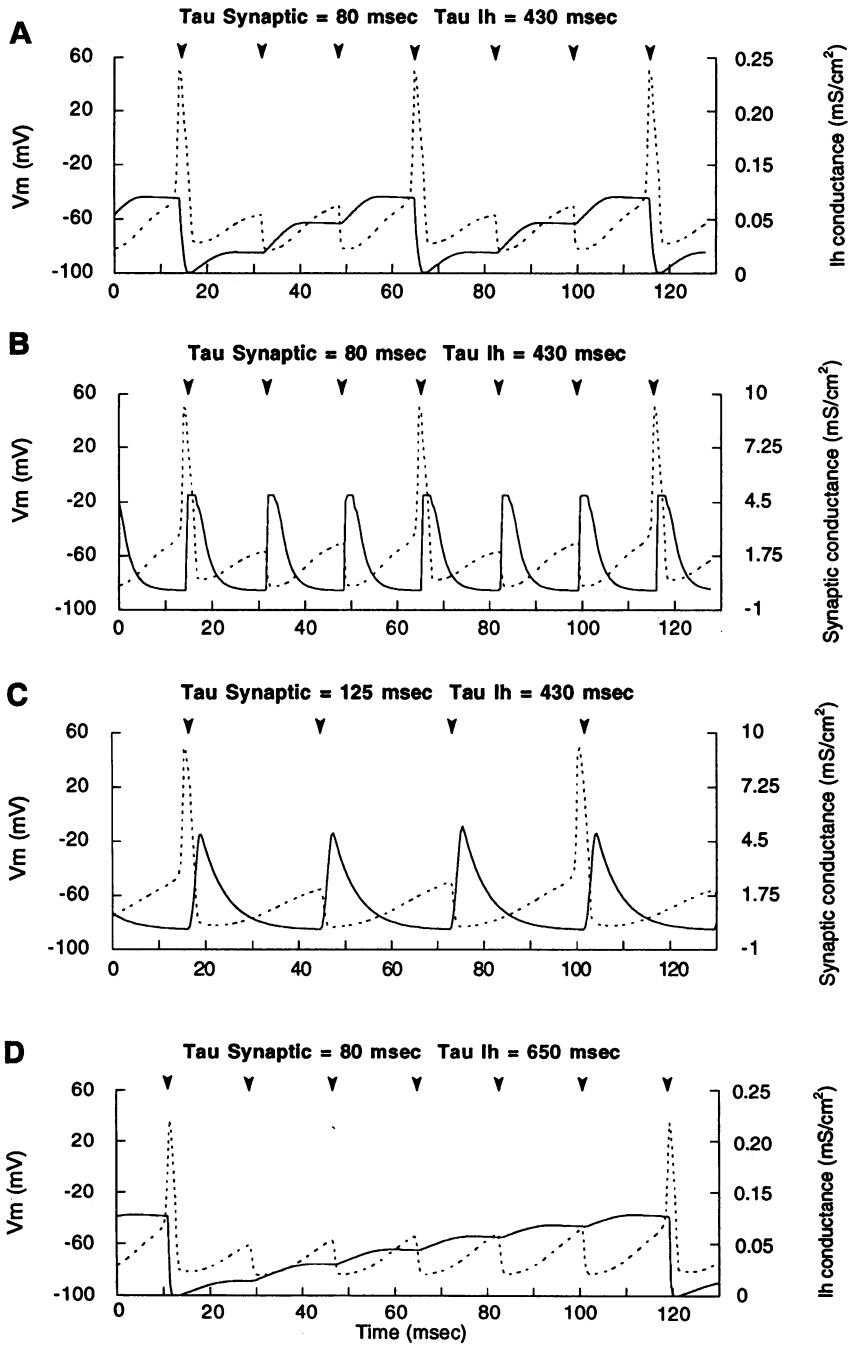

FIG. 2. Conductance vs. time in an E-cell of the reduced network of the i_h and synaptic current from the I-cell. In each case, dotted curve is membrane potential vs. time. (*A*) i_h conductance vs. time, with i_h time constant set to 430 msec at −70 mV. Synaptic time constant is 80 msec. g_{i_h} = 3 mS/cm² and the half-activation voltage is − 75 mV. (*B*) Synaptic conductance vs. time, using the same parameters as in *A*. (*C*) Synaptic conductance vs. time with the same parameters in *B*, except that the synaptic time constant is set to 125 msec, changing the period of the rhythm. (*D*) i_h conductance vs. time with the same parameters as in *A* except for the i_h kinetics. Curve describing the time constant vs. voltage is multiplied by ≈1.5, so that the time constant at −70 mV is 650 msec. The E-cell now fires after six cycles instead of every three cycles, while the population rhythm changes very little.

i_h changes the fraction of cycles that a given E-cell fires without significantly changing the periodicity of the rhythm.

In other simulations in this network (not reported here) we have shown that, as the i_h time constant is changed, the population period changes slowly, but the period of a single cell changes abruptly (thus changing its entrainment mode with the population cycle from 1:1 to 1:2 to 1:3). By contrast, change in the synaptic kinetics over the same range (20-fold) changes the period of the population but leaves the entrainment mode constant.

Discussion

Properties of the Network. Rhythmicity is a property of very simple networks having at least 1 E- and 1 I-cell. In a network that has a cortex-like architecture of extensive convergence and divergence, a population rhythm does not require that each E–I pair be capable of oscillating. The convergence of the network allows each cell to receive input provided that enough of the cells have fired in the previous cycle. The convergence and divergence together ensure that there is roughly the same periodic input to all the cells of the subpopulations.

In our network, the currents were set so that the excitatory postsynaptic potential (EPSP) from any E-cell is sufficient to cause an I-cell to fire. This was needed because the number of cells in our network was relatively small. For a network of appropriate physiological size, and with sufficient convergence and divergence, we expect that the phenomena persist even if the firing of an I-cell requires many EPSPs.

The mechanism described here produces regulation of population frequency, while the amplitude of the field potential is modulated. One reason is that the time interval between an I-cell action potential and the next round of E-cell action potentials depends very little on the average number of cells in the network that are firing in a given cycle. Rather, the network provides E-cells with a window of opportunity within which to fire. The time between E-cell action potentials is governed mainly by the time constant of the synaptic

inhibition, while the length of the window, which is much shorter, is governed by the interval between E-cell firing and I-cell firing plus the rapid buildup of inhibition. Those cells with high enough i_h to fire upon release of inhibition in a given window do so; the others wait for the next cycle. Thus, in spite of distribution of parameters within the population, those cells that do fire in a given cycle are almost synchronous, giving a sharp population rhythm. The number of cells firing is modulated by changing the maximal conductance of i_h or the position of its activation curve. The larger the network, the greater the range of possible amplitude modulation. With a 50% change in average maximal conductance in the 55-cell network, we obtained a 48% change in amplitude of the field potential, and a 6% change in the frequency. For the 7-cell network, the 50% change in maximal conductance led to a 23% change in field potential amplitude and a 10% change in frequency.

For large networks, we have found that the rhythmic behavior is not robust when the maximal conductance of i_h is set uniformly for the E-cells. The difficulty is the prevention of too large a degree of synchrony among the cells; if too many cells fire in a given cycle, those cells are unavailable for firing until their level of i_h builds up again, and the network crashes because not enough I-cells get input in the next cycle. One way to prevent the unwanted synchrony uses a distribution of maximal i_h conductances for the E-cells. Then the E-cells build up to firing at different rates, and those cells that have fired in one cycle become ready to fire again at a mixture of later cycles.

The rhythmic behavior and sparse firing of cells is robust to variations in time constants, including those of the I–E and E–I connections and the i_h current. When the E–I time constants are varied (up to 30%) in the population, the E-cells remain synchronous, while there is a small spread (much less than the spread in time constants) in the firing time and spike duration of the I-cells. When the I–E time constants are allowed to vary (up to 25%) over the population, both the E-cells and the I-cells remain synchronous (when they fire in a given cycle); the major effect is that the cycle time is less regular cycle to cycle. Variation in kinetics of i_h has essentially the same effect as variation in maximal conductance of that current.

Related Models. Most models of cortical activity either use very simple elements, in which the variables are averaged firing rates (18, 19) or phases for oscillatory elements (24, 25), or are very detailed and large simulations using thousands of elements with layers of complexity that include many ionic and synaptic currents with many time scales as well as spatial dependence of the connections (26, 27). The above simulation is intended to draw attention to the functional possibilities associated with particular ionic currents without modeling the details of neural activity.

For models of the hippocampus and the thalamus that reproduce some of the features of this paper see refs. 16 and 28–31. Asynchronous states in networks have been produced in various other models (32, 33) (D. Terman, personal communication); none of these models is concerned with the potential role of particular ionic currents. Other models using currents including or similar to i_h are described in refs. 34 and 35. The ability of inhibition to produce synchronization of some cells, as in our method, was also noted (36).

Biological Significance. i_h is known to exist in some parts of the brain that produce rhythmic activity and that have networks of excitatory and inhibitory cells interacting through convergent and divergent connections. One such example is the network of relay cells and nucleus reticularis cells within the thalamus (1). Population phenomena similar to those discussed in this paper are associated with the generation of spindle waves *in vivo* (14) as well as in a slice preparation (15). We note that the mechanism of this paper produces synchrony among the subset of excitatory cells that fire in any cycle, even though there are no direct connections among those cells; this is also true of the excitatory elements of this intrathalamic network, the relay cells (37).

Another potentially relevant network is that formed by the relay cells in the thalamus giving inhibition to cortical cells and excitation from the latter cells back to the relay cells (1). Oscillations are found in the 30- to 50-Hz range during attention and cognition (38), and it has been suggested that the thalamus may be involved in the production of these rhythms (1).

Cells in the thalamus and in the cortex have many conductances in addition to the ones represented in our model (1). It is possible that other slow conductances, such as a slowly inactivating calcium-gated potassium current, could produce similar phenomena, in which an easily modulatable quantity (like the i_h activation curve) dramatically modifies amplitude while preserving the population frequency. It remains to be fully understood what combinations of currents and time scales display this regulation, thus allowing the population rhythm and the microcircuits to be used for different tasks. We note that the larger the network, the sparser the involvement of any individual component can be and, hence, the more flexibly the network may "multiplex."

The model in this paper does not deal with spatial differences in connectivity. However, if there are such differences, and different regions have different average levels of i_h conductances or hyperpolarization, then the network can have spatial differences in field potential amplitude while having a uniform "carrier wave" frequency. The existence of field potentials with these properties has been noted by Freeman (20). The mechanism of this paper could also be used to help facilitate "map overlays" of different modalities in the cortex. That is, information from, e.g., the auditory cortex could, via the thalamus, be relayed to the visual cortex without disturbing aspects of the visual processing.

Appendix

The equations used for both the E-cells and the I-cells were Hodgkin–Huxley equations

$$C\frac{dV}{dt} = -\Sigma \text{ ionic currents.} \qquad \text{[A1]}$$

For the E-cell, the RHS of [A1] is $i_{Na} + i_K + i_h + i_{leak} + i_{syn}$

$$i_{Na} = \bar{g}_{Na} m^3 h^2 [V - E_{Na}],$$

where

$$\tau_m(V)\frac{dm}{dt} = m_\infty(V) - m,$$

$$\tau_h(V)\frac{dh}{dt} = h_\infty(V) - h,$$

and

$$m_\infty(V) = 1 - \left[\frac{1}{1 + \exp\left(\frac{-31 - V}{-10}\right)}\right],$$

$$h_\infty(V) = 1 - \left[\frac{1}{1 + \exp\left(\frac{V + 45}{-7}\right)}\right],$$

$$\tau_m(V) = \frac{0.57}{\left[\exp\left(\frac{V+40}{58}\right) + \exp\left(\frac{23-V}{15}\right)\right]},$$

$$\tau_h(V) = 72\left[\left(\frac{1}{1+\exp\left(\frac{-26-V}{17}\right)}\right)\left(\frac{1}{1+\exp\left(\frac{V+47}{8.7}\right)}\right)\right]$$

$$i_K = \bar{g}_K n_K^4 (V - E_K),$$

where

$$\tau_K(V)\frac{dn_K}{dt} = n_{K,\infty}(V) - n_K,$$

$$n_{K,\infty}(V) = 0.96 - \left[\frac{1}{1+\exp\left(\frac{-46-V}{-17}\right)}\right],$$

$$\tau_K(V) = 9.4\left[\left(\frac{1}{1+\exp\left(\frac{-104-V}{17}\right)}\right) \times \left(\frac{1}{1+\exp\left(\frac{V+44}{33}\right)}\right)\right]$$

$$i_h = \bar{g}_{i_h} n_{i_h} (V - E_{i_h}),$$

where

$$\tau_{i_h}\frac{dn_{i_h}}{dt} = n_{i_{h,\infty}}(V) - n_{i_h},$$

$$n_{i_{h,\infty}}(V) = \left[\frac{1}{1+\exp\left(\frac{V+75}{4.3}\right)}\right] - 0.06,$$

$$\tau_{i_h}(V) = \left[\frac{631}{1+\exp\left(\frac{V+2.9}{4.2}\right)}\right] - 214$$

$$i_{leak} = \bar{g}_{leak}(V - E_{leak})$$

$$i_{syn} = \bar{g}_{syn} n_s (V - E_{syn}),$$

where

$$\tau_s\frac{dn_s}{dt} = n_{s,\infty}(V) - n_s,$$

$$n_{s,\infty}(V) = \left[\frac{1.4}{1+\exp\left(\frac{-23-V}{6.2}\right)}\right] - 0.43.$$

The above activation and kinetic functions were constructed by using curve-fitting programs, and the constants given are approximate. Gating variables and time constants are set to zero by the software if the above equations give negative values. The I-cell had all of the above currents except for i_h, and the forms of the equations used were the same as above. The equations for the E-cells and I-cells differed in the constants used for the maximal conductances, time constants, and reversal potentials. For the E-cells, the constants were given by $C = 1\ \mu F/cm^2$, $\bar{g}_K = 20$, $E_K = -72$, $\bar{g}_{Na} = 120$, $E_{Na} = 55$, $E_{i_h} = -10$, $\bar{g}_{leak} = 0.3$, $E_{leak} = -50$, $\bar{g}_{syn} = 0.6$, $E_{syn} = 55$, $\tau_s = 20$ msec. The units for maximal conductance and reversal potential are mS/cm^2 and mV. For the I-cells, the constants were the same for C, i_K, and i_{Na}: $\bar{g}_{leak} = 0.1$, $E_L = -60$, $\bar{g}_{syn} = 2.1$, $E_{syn} = -85$, $\tau_s = 80$ msec.

The software used to produce the simulations was developed by G.L. and is not commercially available. The numerical method used in the software is the exponential method (39), a first-order method often applied to neural models because of its good stability properties. The numerical results were partially checked by the Runge–Kutta method.

We wish to thank T. Bal and R. Traub for useful conversations and E. Marder for much help in the production of this paper. The research of N.K. was partially supported by National Institute of Mental Health (NIMH) Grant MH47150. The research of G.L. was partially supported by NIMH Grant MH46742 to E. Marder.

1. McCormick, D. A. (1992) *Prog. Neurobiol.* **39**, 337–338.
2. Spain, W. J., Schwindt, P. C. & Crill, W. E. (1987) *J. Neurophysiol.* **57**, 1555–1576.
3. McCormick, D. A. & Pape, H.-C. (1990) *J. Physiol.* **431**, 291–318.
4. Soltesz, I., Lightowler, S., Leresche, N., Jassik-Gerschenfeld, D., Pollard, C. E. & Crunelli, V. (1991) *J. Physiol.* **441**, 175–197.
5. McCormick, D. A. & Williamson, A. (1991) *J. Neurosci.* **11**, 3188–3199.
6. McCormick, D. & Pape, H.-C. (1990) *J. Physiol.* **431**, 319–342.
7. Tokimasa, T., Sugiyama, K., Akasu, T. & Muteki, T. (1990) *Br. J. Pharmacol.* **101**, 190–192.
8. Pape, H.-C. & Mager, R. (1992) *Neuron* **9**, 441–448.
9. Tokimasa, T. & Akasu, T. (1990) *J. Physiol.* **420**, 409–429.
10. Kamondi, A. & Reiner, A. (1991) *J. Neurophysiol.* **66**, 1902–1911.
11. Hwa, G. & Avoli, M. (1991) *Neurosci. Lett.* **124**, 65–68.
12. Foehring, R. C. & Waters, R. S. (1991) *Neurosci. Lett.* **124**, 17–21.
13. Basar, E. & Bullock, T. H., eds. (1992) *Induced Rhythms in the Brain* (Birkhäuser, Boston).
14. Steriade, M. & Deschenes, M. (1984) *Brain Res. Rev.* **8**, 1–63.
15. von Krosigk, M., Bal, T. & McCormick, D. A. (1993) *Science* **261**, 361–364.
16. Traub, R. D., Miles, R. & Wong, K. S. (1989) *Science* **243**, 1319–1325.
17. Perkel, D. H. & Mulloney, B. (1974) *Science* **185**, 181–183.
18. Wilson, H. R. & Cowan, J. D. (1972) *Biophys. J.* **12**, 1–24.
19. Ermentrout, G. B. & Cowan, J. D. (1979) *J. Math. Biol.* **7**, 265–280.
20. Freeman, W. J. (1975) *Mass Action in the Nervous System* (Academic, New York).
21. LoFaro, T., Kopell, N., Marder, E. & Hooper, S. (1994) *Neural Comput.* **6**, 69–84.
22. LoFaro, T. (1994) Ph.D. thesis (Boston Univ.).
23. Wang, X.-J. (1994) *Neuroscience* **59**, 21–31.
24. Kammen, D. M., Holmes, P. J. & Koch, C. (1989) in *Models of Brain Function*, ed. Cotterill, R. M. J. (Cambridge Univ. Press, Cambridge, U.K.).
25. Sompolinsky, H., Golomb, D. & Kleinfeld, D. (1991) *Phys. Rev. A* **43**, 6990–7011.
26. Traub, R. D. & Miles, R. (1991) *Neuronal Networks of the Hippocampus* (Cambridge Univ. Press, Cambridge, U.K.).
27. Wilson, M. & Bower, J. (1992) *J. Neurophysiol.* **67**, 981–995.
28. Pinsky, P. F. & Rinzel, J. (1994) *J. Comput. Neurosci.* **1**, 39–60.
29. Golomb, D. & Rinzel, J. (1993) *Phys. Rev. E* **48**, 4810–4814.
30. Golomb, D. & Rinzel, J. (1994) *Physica D (Amsterdam)* **72**, 259–282.
31. Golomb, D., Wang, X.-J. & Rinzel, J. (1994) *J. Neurophysiol.*, in press.
32. Ermentrout, G. B. (1992) *Neural Networks* **5**, 415–431.
33. Abbott, L. & van Vreeswijk, C. (1993) *Phys. Rev. E* **2**, 1483–1490.
34. Wang, X. J. & Rinzel, J. (1992) *Neural Comput.* **4**, 84–97.
35. McCormick, D. A. & Huguenard, J. (1992) *J. Neurophys.* **68**, 1384–1400.
36. Lytton, W. & Sejnowsky, T. (1992) *J. Neurophysiol.* **66**, 1059–1097.
37. Jones, E. G. (1985) *The Thalamus* (Plenum, NY).
38. Gray, C. M. & Singer, W. (1989) *Proc. Natl. Acad. Sci. USA* **86**, 1698–1702.
39. MacGregor, R. J. (1987) *Neural and Brain Modeling* (Academic, San Diego).